Braz J Phys (2015) 45:36–40
DOI 10.1007/s13538-014-0283-x

CONDENSED MATTER

Microstructural Properties of Chemically Synthesized Cubic ZnS Nanocrystals

Kuldeep Deka · M. P. C. Kalita

Received: 18 September 2014 / Published online: 4 December 2014

Abstract In this paper we present microstructural properties of chemically synthesized cubic zinc sulfide (ZnS) nanocrystals, investigated by X-ray diffraction (XRD) line profile analysis applying classical Williamson-Hall (WH) and modified Williamson-Hall (MWH) methods, and transmission electron microscopy (TEM) observations. ZnS nanocrystals are synthesized using 1:1 M ratio of Zn and S precursors with 25, 50, and 75 mM, 2-mercaptoethanol as capping agent. WH analyses show that the average crystallite sizes (lattice strain) are 3.98 nm (2.22×10−2), 2.69 nm (1.99×10−2), and 2.58 nm (2.65×10−2). Dislocation contrast factors of ZnS crystals required for the MWH method are calculated from their elastic stiffness constants for various proportions of screw and edge dislocations. The best fit to MWH equation is found to be for dislocation contrast factors corresponding to 100 % edge dislocations and thereby suggesting edge dislocations are main contributors to strain. MWH analyses show dislocation density of 3.65, 2.69, and 2.47 nm crystallites are 3.19×10^{18} m^{-2}, 2.58×10^{18} m^{-2}, and 4.62×10^{18} m^{-2}, respectively. The crystallite sizes as estimated from the WH, MWH, and TEM studies are found to be intercorrelated. Presence of edge dislocations, as suggested by the MWH analysis, is confirmed by high resolution TEM (HRTEM) studies.

Keywords Dislocation · Lattice strain · ?Modified Williamson-Hall · X-ray diffraction · ?ZnS nanocrystals

K. Deka · M. P. C. Kalita (✉)
Department of Physics, Gauhati University, Guwahati, Assam 781014, India
e-mail: manoskalita@gmail.com

1 Introduction

In recent years, various nanocrystalline (NC) materials were widely investigated from both fundamental and application points of view. Properties of NC materials changes drastically and often leads to novel properties different from their bulk form. Size dependent optical [1–3] and magnetic [3] properties, enhanced catalytic properties of nanocrystals [4, 5] are examples of some well-known properties of NC materials. Presence of lattice strain in nanocrystals is also well established [6–8]. Along with small sizes, strain also affects the properties of nanocrystals. Strain increases the coercivity of magnetic materials [8, 9], optical and electronic properties of semiconductors can be tuned by strain [10, 11], and catalytic properties can be changed by strain [12]. In order to understand the various properties of nanocrystals, different structural aspects must be considered and proper estimation of structural parameters like crystallite size, lattice strain, and dislocation density are important. Zinc sulfide (ZnS) is a group II–VI wide band gap semiconductor and is a promising material for a wide range of applications like light emitting diodes, electroluminescence, flat panel displays, infrared windows, sensors, lasers etc. [13, 14]. ZnS can exist in different crystalline structures viz. cubic zinc blende, hexagonal wurtzite, and rarely observed cubic rock salt [15, 16]. In bulk ZnS, cubic zinc blende is the most stable phase at room temperature which transforms to hexagonal wurtzite at 1020 °C [17]. However, in nanocrystals of ZnS, the relative stability of the two phases changes and low temperature synthesis of hexagonal wurtzite ZnS nanocrystals was recently reported [18]. Synthesis of ZnS nanocrystals with desired crystal structure is of great importance at present. In the present work, ZnS nanocrytsals with cubic zinc blende structure were synthesized by a room temperature chemical coprecipitation method. A detailed analysis of microstructural properties of the ZnS nanocrystals is carried out by X-ray

diffraction (XRD) line profile analysis, applying the Williamson-Hall (WH), modified Williamson-Hall (MWH) methods, and transmission electron microscopy (TEM) observations are presented.

2 Experimental Details

For the synthesis of ZnS nanocrystals with 2-mercaptoethanol as capping agent, required amount of zinc chloride and sodium sulfide are dissolved in 20 ml triple distilled water separately; 0.25, 0.50, and 0.75 mL 2-mercaptoethanol are mixed with 143 mL triple distilled water to obtain 25, 50, and 75 mM 2-mercaptoethanol solutions, respectively. The solutions are mixed together and kept at room temperature for 48 h and then the precipitates are filtered, and washed in triple distilled water and then allowed to dry for a few days. All the samples are obtained as powders and they are characterized by X-ray diffractometer (Rigaku, TTRAX-III) with CuK_α radiation. The ZnS powders with 75 mM 2-mercaptoethanol are characterized by transmission electron microscope (JEM-2100, Jeol).

3 Results and Discussion

3.1 X-ray Diffraction Results and Analysis

Figure 1 shows XRD patterns of ZnS powders with 2-mercaptoethanol concentrations of 25, 50, and 75 mM. The XRD patterns are found to be in good agreement with standard pattern of bulk ZnS face-centered cubic crystal (JCPDS data file: 05–0566). The XRD patterns indicate the samples are well crystallized. The diffraction lines are indexed as (111), (220), and (311) reflections of ZnS.

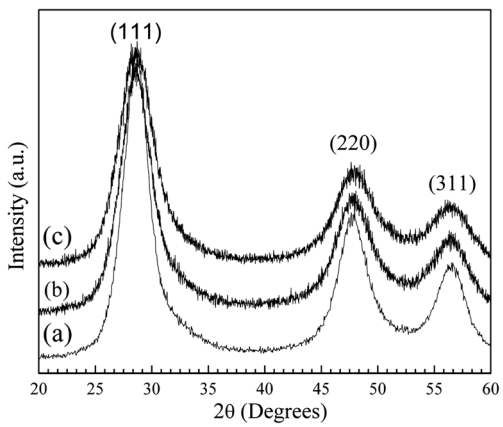

Fig. 1 XRD pattern of ZnS nanocrystals with 2-mercaptoethanol concentrations of 25 mM (**a**), 50 mM (**b**), and 75 mM (**c**)

3.2 XRD Analysis by Classical Williamson-Hall Method

The diffraction lines are broad, indicating formation of crystals with small crystallite size, having lattice strain. If these two contributions are represented by Gaussian curves, then according to the WH method [19, 20]

$$(\Delta K)^2 = \left(\frac{0.9}{D}\right)^2 + 4e^2K^2 \quad (1)$$

where $\Delta K = \cos\theta\,\Delta\theta/\lambda$ $\Delta\theta$ is the FWHM of the diffraction lines, 2θ is the scattering angle, λ is the wavelength of CuK_α radiation (0.15406 nm), $K = 2\sin\theta/\lambda$, D is average crystallite size, and e is the lattice strain. All the X-ray diffraction lines in Fig. 1 are used to construct a linear plot between $(\Delta K)^2$ and K^2 (presented in Fig. 2), and the average crystallite size and lattice strain are calculated using equation (1) (presented in Table 2). The average crystallite sizes (lattice strain) are found to be 3.98 nm (2.22×10^{-2}), 2.69 nm (1.99×10^{-2}), and 2.58 nm (2.65×10^{-2}) for 2-mercaptoetanol concentrations of 25, 50, and 75 mM, respectively. Thus, the WH analysis shows formation of strained nanocrystals.

3.3 XRD Analysis by Modified Williamson-Hall Method

Assuming that strain is due to creation of dislocations, the X-ray diffraction results are analyzed by the MWH method [8, 9, 20–24]. According to the MWH method, the equation (1) can be written as

$$(\Delta K)^2 = \left(\frac{0.9}{D}\right)^2 + \left(\frac{\pi b^2 \rho}{2B}\right)K^2C_{hkl} \quad (2)$$

where D is average crystallite size, ρ is the average dislocation density, b is the modulus of Burger vector of dislocation (for f.c.c. crystals $b = \frac{a}{\sqrt{2}}$ where a is lattice parameter), C_{hkl} is the

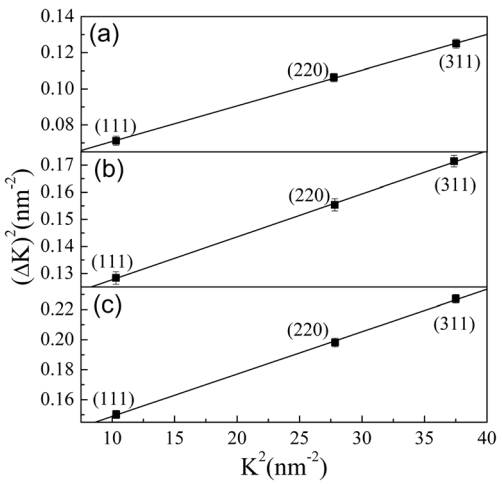

Fig. 2 WH plots for ZnS nanocrystals with 2-mercaptoethanol concentrations of 25 mM (**a**), 50 mM (**b**), and 75 mM (**c**)

dislocation contrast factor for the (hkl) Bragg reflection, and B is a constant that can be taken as 10 for a wide range of dislocation distribution [24].

The contrast factor C_{hkl} is related to the contrast factor for Bragg reflection (h00) as given by the equation [22, 23]

$$C_{hkl} = C_{h00}\left(1-qH^2\right) \quad (3)$$

where $H^2=(h^2k^2+h^2l^2+k^2l^2)/(h^2+k^2+l^2)^2$ for cubic crystals and q is a parameter which depends on the elastic constants and type of dislocations. The C_{h00} and q values for screw and edge dislocations can be obtained using the relations [22, 23]

$$C_{h00} = a[1-\exp(-Ai/b)] + cAi + d, \quad (4)$$

$$q = a_1[1-\exp(-Ai/b_1)] + c_1Ai + d_1. \quad (5)$$

Ai is the elastic anisotropy constant given as

$$Ai = 2C_{44}/(C_{11}-C_{12}) \quad (6)$$

where C_{11}, C_{12}, and C_{44} are elastic stiffness constants; a, b, c, and d in equation (4) and a_1, b_1, c_1, and d_1 in equation (5) are parameters which depend on the type of dislocations and may depend on the elastic constant ratio C_{12}/C_{44}. In case of screw dislocations in f.c.c. crystals, a=0.1740, b=1.9522, c=0.0293, d=0.0662, and a_1=5.4252, b_1=0.7196, c_1=0.0690, d_1=−3.1970 and independent of C_{12}/C_{44} [23]. For edge dislocations in f.c.c. crystals, the values of a, b, c, d and a_1, b_1, c_1, d_1 depend on C_{12}/C_{44} and were reported for the C_{12}/C_{44} values 0.5, 1, 2, and 3 [23]. The elastic stiffness constants of ZnS are C_{11}=104, C_{12}=65 and C_{44}=46.2 GPa [25]. The value of Ai as calculated from equation (6) is 2.3692. The C_{12}/C_{44} ratio for ZnS is 1.4069.

The values of C_{h00} and q for screw dislocations corresponding to the value of Ai=2.3692 are obtained using equations (4) and (5) and are found to be C_{h00}=0.2579 and q=2.1899. For calculating the values of C_{h00} and q for edge dislocations, the values of a,b,c,d and a_1,b_1,c_1,d_1 are obtained by interpolation of their reported values corresponding to C_{12}/C_{44}=1.4069. Thereby, a=0.1981, b=2.1722, c=0.0185, d=0.0882, and a_1=5.2104, b_1=0.8446, c_1=0.0872, d_1=−3.7830 are obtained. The values of C_{h00} and q for edge dislocations corresponding to these values of a,b,c,d and a_1,b_1,c_1,d_1 and Ai=2.3692 are calculated using equations (4) and (5) and found to be C_{h00}=0.2635 and q=1.3185. From the values of C_{h00} and q for pure screw and edge dislocations, C_{hkl} for various reflections are calculated using equation (3). C_{hkl} for various contributions from screw and edge dislocations are calculated and presented in Table 1. Using these values of C_{hkl} plots between $(\Delta K)^2$ and K^2C_{hkl} according to equation (2) are constructed and typical plots for ZnS powders of 75 mM 2-mercaptoethanol concentration are presented in Fig. 3. The best linear fit is obtained for 0 % screw dislocations and 100 % edge dislocations. It shows that dislocations present in the ZnS nanocrystals are of edge-type and thereby indicates that edge dislocations are main contributors in inducing strain in the nanocrystals. Similar results are obtained for the ZnS powders with 25 and 50 mM 2-mercaptoethanol concentrations. The average crystallite size and average dislocation density are calculated and presented in Table 2.

Table 1 Average dislocation contrast factors C_{hkl} of the Bragg reflections of ZnS

Percentage of screw (S) and edge (E) dislocations	C_{111}	C_{200}	C_{220}	C_{311}
100 % S 0 % E	0.0698	0.2579	0.1167	0.1692
50 % S 50 % E	0.1088	0.2607	0.1467	0.1891
25 % S 75 % E	0.1283	0.2621	0.1616	0.1990
0 % S 100 % E	0.1478	0.2635	0.1766	0.2089

Table 2 Average crystallite size, lattice strain, and dislocation density of ZnS nanocrystals

Samples ZnS 2-mercaptoethanol concentration (mM)	Crystallite size (nm) WH method	Crystallite size (nm) MWH method	Lattice strain ($\times10^{-2}$) WH method	Dislocation density ($\times10^{18}$ m^{-2}) MWH method
25	3.98±0.14	3.65±0.09	2.22±0.07	3.19±0.20
50	2.69±0.04	2.69±0.03	1.99±0.10	2.58±0.19
75	2.58±0.04	2.47±0.03	2.65±0.08	4.62±0.19

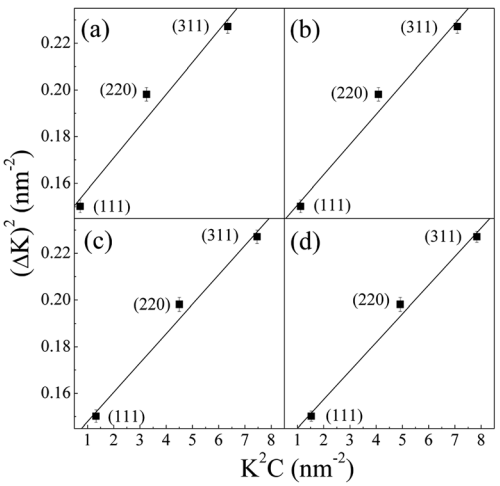

Figure 3 MWH plots for ZnS nanocrystals with 75 mM 2-mercaptoethanol, considering various proportions of screw (*S*) and edge (*E*) dislocations: 100 % S 0 % E (**a**), 50 % S 50 % E (**b**), 25 % S 75 % E (**c**), and 0 % S 100 % E (**d**)

4 Transmission Electron Microscopy Results and Analysis

Figure 4a shows the TEM micrograph of ZnS nanocrystals prepared using 75 mM 2-mercaptoethanol concentration and in the inset, the selected area electron diffraction (SAED) pattern is presented. Distinct rings in the SAED patterns shows formation of polycrystalline ZnS. The rings are indexed as (111), (220), and (311) reflections of ZnS. The TEM micrograph shows agglomerated morphology of the nanocrystals typical of polycrystalline materials. High resolution TEM (HRTEM) measurements are carried out for investigating the size of the crystallites, possible presence of lattice strain, and dislocations. The HRTEM results are presented in Fig. 4b. The encircled areas in the figure shows crystallites, and the size is found to be about 3 nm, which is in good agreement with the results obtained by the WH and MWH analysis. The encircled areas in Fig. 4b are shown in magnified form in the insets. Figure 4b (i, ii) show edge-type dislocations. Thus, presence of edge-type dislocation, as predicted by the MWH analysis, is confirmed by the HRTEM observations. In Fig. 4b (iii, iv), it can be seen that the interplanar spacing has increased while in Fig. 4b (vi) show areas of decreased interplanar spacing, indicating presence of nonuniform strain at the boundaries of the crystallites. The presence of strain in the boundaries of crystallites can be due to stress field induced by excess volume in the boundaries [6]. Thus, edge dislocations along with stress field in the boundaries contribute to the origin of strain in the presently investigated ZnS nanocrystals.

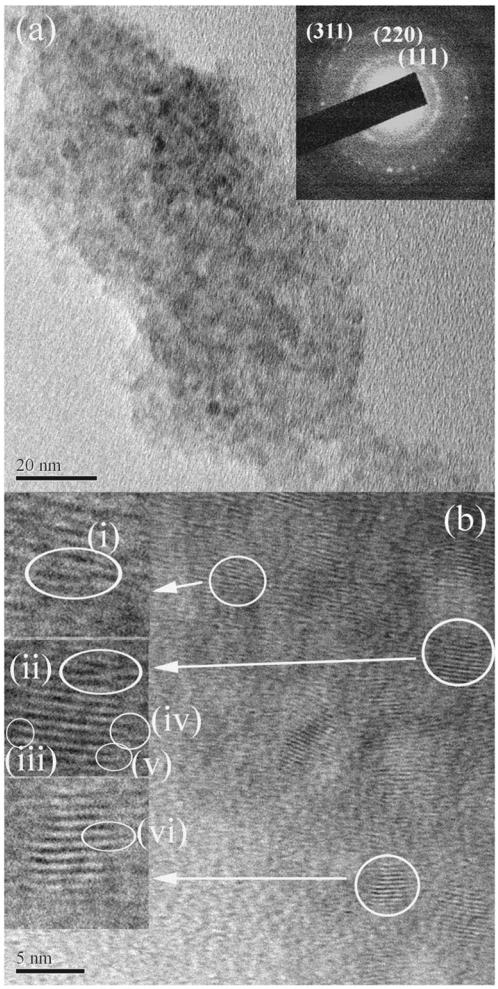

Fig. 4 **a** TEM images and SAED pattern and **b** HRTEM images of ZnS nanocrystals with 75 mM 2-mercaptoetanol concentration

5 Conclusion

In summary, ZnS nanocrystals with cubic zinc blende crystal structure have been synthesized by a room temperature chemical coprecipitation method, using various concentrations of 2-mercaptoethanol as capping agent. Microstructural studies were carried out by XRD line profile analysis, applying the WH and MWH methods, and TEM observations. The crystallite sizes, as estimated from the WH, MWH, and TEM studies are found to be intercorrelated. The WH analysis shows presence of strain while the MWH analysis suggests that edge dislocations are main contributors to lattice strain. Presence of edge dislocations is confirmed by the HRTEM studies. With increasing concentration of 2-mercaptoethanol, decrease of crystallite size was observed, showing the importance of 2-mercaptoethanol in controlling the size of the nanocrystals.

Acknowledgments This work was supported by DST, India vide project no SB/FTP/PS-008/2013. We thank the Department of Physics, IITG for providing XRD facility and SAIF, North-Eastern Hill University, Shillong for providing the TEM facility.

References

1. M. Nirmal, B.O. Dabbousi, M.G. Bawendi, J.J. Macklin, J.K. Trautman, T.D. Harris, L.E. Brus, Nature **383**, 802 (1996)
2. S Kan, T. Mokari, E. Rothenberg, U. Banin, Nature Mater. 2, 155 (2003).
3. D. Vollath, *Nanomaterials: an introduction to synthesis, properties and applications*, 2nd edn. (Wiley-VCH, Weinheim, Germany, 2013)
4. C. Burda, X. Chen, R. Narayanan, M.A. El-Sayed, Chem. Rev. **105**, 1025 (2005)
5. C.N.R. Rao, G.U. Kulkarni, P.J. Thomas, P.P. Edwards, Chem. Eur. J. **8**, 28 (2002)
6. W. Qin, J.A. Szpunar, Phil. Mag. Lett. **85**, 649 (2006)
7. M.P.C. Kalita, K. Deka, J. Das, N. Hazarika, P. Dey, R. Das, S. Paul, T. Sarmah, B.K. Sarma, Mater. Lett. **87**, 84 (2012)
8. T.D. Shen, R.B. Schwarz, J.D. Thompson, Phys. Rev. B **72**, 014431 (2005)
9. M.P.C. Kalita, A. Perumal, A. Srinivasan, J. Phys. D Appl. Phys. **42**, 105001 (2009)
10. A.M. Smith, A.M. Mohs, S. Nie, Nature Nanotech. **4**, 56 (2009)
11. N. Pote, C. Phadnis, K. Sonawane, V. Sudarsan, S. Mahamuni, Sol. Stat. Comm. **192**, 6 (2014)

12. C.H. Kuo, L.K. Lamontagne, C.N. Brodsky, L.Y. Chou, J. Zhuang, B.T. Sneed, M.K. Sheehan, C.K. Tsung, Chem. Sus. Chem. **6**, 1993 (2013)
13. X. Fang, T. Zhai, U.K. Gautam, L. Li, L. Wu, Y. Bando, D. Golberg, Prog. Mater. Sci. **56**, 175 (2011)
14. S. Cholan, N. Shanmugam, N. Kannadasan, K. Sathishkumar, G. Viruthagiri, Mater. Resear. Exp. **1**, 025010 (2014)
15. F.A. La Porta, L. Gracia, J. Andres, J.R. Sambrano, J.A. Varela, E. Longo, J. Am, Ceram. Soc. (2014). doi:10.1111/jace.13191
16. F.A. La Porta, M.M. Ferrer, Y.V.B. de Santana, C.W. Raubach, V.M. Longo, J.R. Sambrano, E. Longo, J. Andres, M.S. Li, J.A. Varela, J. All. Comp. **556**, 153 (2013)
17. F.A. La Porta, J. Andres, M.S. Li, J.R. Sambrano, J.A. Varela, E. Longo, Phys. Chem. Chem. Phys. **16**, 20127 (2014)
18. S.A. Acharya, N. Maheswari, L. Tatikondewar, A. Kshirsagar, S.K. Kulkarni, Cryst. Growth Des. **13**, 1369 (2013)
19. G.K. Williamson, W.H. Hall, Acta Metall. **1**, 22 (1953)
20. J. Gubicza, J. Szepvolgyi, I. Mohai, G. Ribarik, T. Ungar, J. Mater. Scien. **35**, 3711 (2000)
21. T. Ungar, A. Borbely, Appl. Phys. Lett. **69**, 3137 (1996)
22. T. Ungar, G. Tichy, Phys. Stat. Sol. A **171**, 425 (1999)
23. T. Ungar, I. Dragomir, A. Revesz, A. Borbely, J. Appl. Cryst. **32**, 992 (1999)
24. A. Revesz, T. Ungar, A. Borbely, J. Lendvai, Nanostruct. Mater. **7**, 779 (1996)
25. D. Berlincourt, H. Jaffe, L.R. Shiozawa, Phys. Rev. **129**, 1009 (1963)